Molecular Omics

Delineating Toxicity Mechanisms Associated with MRI Contrast Enhancement through a Multidimensional Toxicogenomic Profiling of Gadolinium

Journal:	*Molecular Omics*
Manuscript ID	MO-RES-07-2021-000267.R1
Article Type:	Research Article
Date Submitted by the Author:	16-Dec-2021

Complete List of Authors:	M. Pallares, Roger; E O Lawrence Berkeley National Laboratory An, Dahlia; E O Lawrence Berkeley National Laboratory Hebert, Solene; E O Lawrence Berkeley National Laboratory, Chemical Sciences Faulkner, David; E O Lawrence Berkeley National Laboratory Loguinov, Alex; University of Florida, Center for Environmental and Human Toxicology Proctor, Michael; University of Florida, Center for Environmental and Human Toxicology Villalobos, Jonathan; E O Lawrence Berkeley National Laboratory Bjornstad, Kathleen; E O Lawrence Berkeley National Laboratory Rosen, Chris; E O Lawrence Berkeley National Laboratory Vulpe, Christopher; University of Florida, Center for Environmental and Human Toxicology Abergel, Rebecca; E O Lawrence Berkeley National Laboratory; University of California Berkeley

Delineating Toxicity Mechanisms Associated with MRI Contrast Enhancement through a Multidimensional Toxicogenomic Profiling of Gadolinium

Roger M. Pallares,[1] Dahlia D. An,[1] Solène Hébert,[1] David Faulkner,[1] Alex Loguinov,[2] Michael Proctor,[2] Jonathan A. Villalobos,[1] Kathleen A. Bjornstad,[1] Chris J. Rosen,[1] Christopher Vulpe,[2] and Rebecca J. Abergel[1,3,*]

Affiliations:

[1]Chemical Sciences Division, Lawrence Berkeley National Laboratory, Berkeley, CA, 94720, USA

[2]Center for Environmental and Human Toxicology, Department of Physiological Sciences, College of Veterinary Medicine, University of Florida, Gainesville, FL, 32611, USA

[3]Department of Nuclear Engineering, University of California, Berkeley, CA, 94720, USA

*E-mail: abergel@berkeley.edu

Abstract:

Gadolinium is a metal used in contrast agents for magnetic resonance imaging. Although gadolinium is widely used in clinical settings, many concerns regarding its toxicity and bioaccumulation after gadolinium-based contrast agent administration have been raised and published over the last decade. To date, most toxicological studies have focused on identifying acute effects following gadolinium exposure, rather than investigating associated toxicity mechanisms. In this study, we employ functional toxicogenomics to assess mechanistic interactions of gadolinium with *Saccharomyces cerevisiae*. Furthermore, we determine which mechanisms are conserved in humans, and their implications for diseases related to the use of

gadolinium-based contrast agents in medicine. A homozygous deletion pool of 4291 strains were screened to identify biological functions and pathways disturbed by the metal. Gene ontology and pathway enrichment analyses showed endocytosis and vesicle-mediated transport as the main yeast response to gadolinium, while certain metabolic processes, such as glycosylation, were the primary disrupted functions after the metal treatments. Cluster and protein-protein interaction network analyses identified proteins mediating vesicle-mediated transport through the Golgi apparatus and the vacuole, and vesicle cargo exocytosis as key components to reduce the metal toxicity. Moreover, the metal seemed to induce cytotoxicity by disrupting the function of enzymes (*e.g.* transferases and proteases) and chaperones involved in metabolic processes. Several of the genes and proteins associated with gadolinium toxicity are conserved in humans, suggesting that they may participate in pathologies linked to gadolinium-based contrast agent exposures. We thereby discuss the potential role of these conserved genes and gene products in gadolinium-induced nephrogenic systemic fibrosis, and propose potential prophylactic strategies to prevent its adverse health effects.

KEYWORDS: gadolinium, gadolinium-based contrast agent, GBCA, toxicity, toxicogenomics.

Introduction

Gadolinium is a metal that stands in the middle of the lanthanide series.[1] As with most lanthanides, it adopts the +3 oxidation state in aqueous solution and tends to form complexes with high coordination numbers (between 8 and 10), primarily through binding with hard-donor oxygen and nitrogen atoms.[1] Gadolinium is paramagnetic at room temperature, and it is used in contrast agents for magnetic resonance imaging (MRI),[2,3] a widely-applied diagnostic tool that often requires additional pharmacological agents to enhance the image contrast.[4] Gadolinium-based contrast agents (GBCAs) can improve the image quality by relaxing water molecules near the metal-ligand complex, helping to clarify the outlines of soft tissue and improving MRI diagnostic performance.[5] Although 25% of MRI procedures employ GBCAs,[6] gadolinium is not a ubiquitous element and several adverse effects have been associated with its use. For instance, there is a strong correlation between GBCA administration and development of nephrogenic systemic fibrosis in patients with renal dysfunction.[7,8] Moreover, gadolinium has been detected in the brain of healthy individuals who received GBCA.[9,10] Consequently, the U.S. Food and Drug Administration has issued a warning regarding retention of gadolinium after administration of GBCA (particularly with linear chelators, as opposed to macrocyclic chelating structures),[11] and the European Medicines Agency has recommended the suspension of another widely-used linear contrast agent, Magnevist, which is the N-methylglucamine salt of the gadolinium complex of diethylenetriamine pentaacetic acid.[12] As a result of these health concerns, new work has focused on improving the detection of gadolinium and GBCAs,[13,14] as well as on developing decorporation protocols to enhance their *in vivo* excretion.[15] Limited research, however, has been performed to understand the molecular origins of gadolinium toxicity: some studies characterized the inhibition growth of model organisms (*e.g.* bacteria, microalga and crustacean) under increasing metal concentrations,[16] while other studies focused on identifying the acute effects after exposure to gadolinium or

GBCAs, *in vivo*.[17,18] To the best of our knowledge, none have studied toxicity molecular mechanisms, which can be explored by genomic-based techniques.

Yeast functional toxicogenomics is a genomic-based tool that allows the characterization of cytotoxic mechanisms through the use of yeast deletion libraries generated by the Yeast Deletion Project, a consortium of researchers across the U.S. and Canada.[19] This strategy uses the differential growth rates among homozygous or heterozygous deletion mutants to infer relationships between genes and fitness upon exposures to metals, pharmaceutical drugs, or other chemicals.[20-23] *Saccharomyces cerevisiae* is one of the best-characterized model organisms because its genome can be easily analyzed by multiple commercial tools. Moreover, as eukaryotes, yeasts share many cellular pathways and biological functions with humans. Hence, functional toxicogenomics not only allows to identify cytotoxicity mechanisms in *S. cerevisiae,* but also to explore potentially-conserved biological features in humans. Nevertheless, the mechanistic information obtained by functional toxicogenomics depends on the experimental conditions, where chemical dose and exposure time have strong effects on the set of genes and paths involved in the cellular response to exposure. Thus, multidimensional studies that systematically screen multiple conditions can identify both universal and condition-specific biological effects.[21]

Here, we report a multidimensional toxicogenomic study that identifies the mechanisms involved in gadolinium interaction with *S. cerevisiae.* The biological effects of the metal were generation dependent, with the yeast response to gadolinium increasing with the number of growth generations. Although only minor disruptions were observed at IC_5 concentrations, a large number of cellular functions were altered at IC_{10} and IC_{20} concentrations. Gene ontology and pathway enrichment analyses indicated that genes and gene products related to endocytosis and vesicle-mediated transport were required for tolerance to the metal. Moreover, gadolinium may promote cytotoxicity by disrupting enzyme and chaperone functions involved in metabolic

processes. Network analysis highlighted several yeast proteins that were conserved in humans, suggesting that they may play a role in human health issues and disease associated with gadolinium and GBCA exposures.

METHODS

Materials

Gadolinium (III) chloride hexahydrate 99%, magnesium (II) chloride 98%, sodium hydroxide 97%, hydrogen chloride 0.1 N and 6 N, sorbitol di-potassium hydrogen phosphate 98%, and potassium phosphate monobasic 98% were purchased from Sigma-Aldrich (St. Louis, MO). Milli-Q water was obtained from Millipore Milli-Q Integral 15 water purification system (Millipore Sigma, Burlington, MA). All metal solutions were prepared in 2 M HCl.

Yeast strains and cultures

Diploid yeast deletion strains (BY4743 background, Life Technologies, Carlsbad, CA) were grown in yeast extract-peptone-dextrose media (YPD, containing 1% yeast extract, 2% peptone, and 2% dextrose) at 30 ˚C with 200 rpm shaking.

For IC_5, IC_{10} and IC_{20} determinations, wild-type yeast was grown to mid-log phase and then diluted to 0.0165 optical density at 600 nm. The gadolinium treatments were added to diluted yeast strains, which were then transferred into different wells in transparent 96-well plates (Grenier Bio-One, Monroe, NC). Plates containing the yeast pools were incubated in a Tecan Genios microplate reader (Tecan Group Ltd., Männedorf, Switzerland) at 30 ˚C with continuous 200 rpm shaking. Optical density of each well at 600 nm was recorded for a period of 24 h in 15 min intervals. The area under the curve was used to calculate the IC_5, IC_{10} and IC_{20} concentrations.

Functional screening of the yeast genome

Homozygous diploid deletion pools (4291 mutants in total) were cultured for 10 and 15 generations in YPD medium at IC_5, IC_{10} and IC_{20} gadolinium concentrations in an automated dispensing system robot built in-house.[24] Forty-eight well plates containing the yeast strains in 700 ml of YPD were continuously shaken and their optical density at 600 nm was recorded in

15 min intervals. To avoid saturation and maintain the yeast in the log phase of growth, at each 5 generations, an inoculant of 23 ml was dispensed by the robot to a fresh well of YPD. After the yeast were grown for 10 or 15 generations, they were dispensed by the robot to a cold plate to inhibit yeast growth, then centrifuged to remove the remaining supernatant, and frozen at -80 ˚C until next protocol step was performed.[24]

The samples were thawed for 10 min, and the yeast pool pellets were re-suspended in autoclaved spheroplast buffer (4.75 g KH_2PO_4, 2.62 g K_2HPO_4, 250 µL 1M $MgCl_2$, and 109.3 g sorbitol), and incubated with 1 mg/ml Zymolyase (Zymo Research, Irvine, CA) for 2 hours at 37 ˚C in order to lyse the cell wall.

DNA was extracted with the Corbett Robotics Xtractor-Gene robot (Qiagen, Hilden, Germany) and Qiagen DX regents. The quality of the extracted DNA was assessed with a NanoQuant module (Tecan, Männedorf, Switzerland), which corroborated that the extracted DNA 260/280 nm ratios were between 1.7 and 2.1 and the oligonucleotide concentrations ranged between 20 and 100 ng/µL.

The extracted DNA was amplified by polymerase chain reaction (PCR), where 22.5 µL of Platinum PCR SuperMix (Thermo Fisher Scientific, Waltham, MA), 5 µL genomic DNA, and 2µL primer mixtures were combined in sealed 96-well plates. The cycle conditions of the PCR program were the following: 95°C / 3min; 25 cycles of 94 °C / 30s, 55 °C / 30s, 72 °C / 30s; followed by 72°C / 10 min and hold at 10°C. After the amplification was finished, the ZR-96 DNA clean and concentrator-5 kit (Zymo Research, Irvine, CA) were employed to purify and concentrate the DNA obtained from the PCR, and the Quant-iT dsDNA Assay Kit (Thermo Fisher Scientific, Waltham, MA) was used to quantify it.

The primers were removed from the DNA solutions by running them for 2 h in a 2% agarose gel, which was then cut in a UV box, and the DNA extracted with GeneJet Gel Extraction Kit

(Thermo Fisher Scientific, Waltham, MA). Lastly, the DNA was sequenced at the Vincent J. Coates Genomics Sequencing Laboratory.

Differential strain sensitivity analysis

Differential strain sensitivity analysis (DSSA) was performed by amplifying the up tag and down tag barcode sequences corresponding to each knockout gene with primers that bind to common regions of the cassette. The readout primers contained adapter sequences from Illumina (San Diego, CA) and a unique 8 base-pair long index sequence that labeled each sample and enabled the multiplexing analysis. Next generation sequencing with an HiSeq 2500 Sequencing System (Illumina, San Diego, CA) was used to count the unique barcodes corresponding to each gene knockout. The FASTQC tool[25] was used to evaluate the sequencing quality and the CASAVA-1.8 filter (Illumina, San Diego, CA) was applied to filter the reads, which were further processed to include only the unique 20 base-pair barcode sequence by employing the FASTX-Toolkit.[26] Biostrings *R* package[27] was used to count reads matching each defined barcode, with the down and up tags being counted separately. Up and down tag Log_2-ratio values were averaged while the corresponding *p*-values were combined using Fisher's method. Counts were normalized and differential barcode abundance analysis between treatment samples and controls based on a negative binomial distribution model was performed with DESeq 2 package.[28] Barcode sequences that were significantly depleted in the treatment compared to the control pool at a given time point (Log_2-ratio value < 0) identified genes whose mutation led to sensitive strains, whereas those that were significantly enriched (Log_2-ratio value > 0) corresponded to genes whose deletion induced increased strain resistance to the treatment. A summary of sensitive and resistant strains was obtained by establishing a cutoff of 0.05 for false discovery rate (FDR) adjusted *p*-values.

Gene ontology analysis, KEEG pathway enrichment analysis, and cluster analysis were performed to the data sets identified by DSSA with the David tool 6.7,[29] setting a *p*-value cutoff of 0.05. FDR was applied to the *p*-values to account for the multiple-hypothesis testing.[30] The analyses were performed for sensitive and resistant mutants separately in order to obtain better biological information. Functional annotation clustering was performed with DAVID 6.7 software, and it relies in Kappa statistics to characterize the degree of common genes between two annotations, and fuzzy heuristic clustering to classify groups with similar annotations according to Kappa values. The software calculates an enrichment score for each group to rank its biological significance. This score is the geometric mean in log scale of the *p*-values of the members in each cluster. Hence, top ranked annotation groups most likely show lower *p*-values for their annotation members. An enrichment score cutoff of 1.0 was set during the analysis. The intracellular localization of the gene products identified in the cluster analysis were screened in the UniProt[31] and Compartments[32] databases. Interactions between gene products identified by DSSA were analyzed by protein-protein interaction network analysis. Caution must be taken when drawing conclusions from protein-protein interaction network analysis, however, as the databases used to draw relationship conclusions are heterogeneous, and may contain errors, which may result in proteins displaying more apparent interactions than in reality. In our case, protein-protein interaction network analysis was performed by mapping DSSA identified strains onto the STRING *S. cerevisiae* functional interaction network (a database considered the gold standard in the field for known and predicted protein-protein interactions).[33] STRING provided a score (ranging from 0.00 to 1.00) for every interaction mapped, which was associated with the likelihood of that interaction being true-positive. We performed the analysis with a score cutoff of 0.90, which was defined as “highest confidence” by the STRING software, and the network was displayed with the edges indicating both functional and physical protein associations.[33] The networks were built only with proteins

identified by DSSA. No higher-order interactions were considered. Lastly, human orthologues of genes associated with gadolinium toxicity were identified with the Alliance of Genome Resources database.[34]

Results and Discussion

Functional profiling of genes required for sensitivity and tolerance to Gadolinium

The concentrations at which wild-type yeast growth was inhibited by 5% (IC_5), 10% (IC_{10}), and 20% (IC_{20}) were initially determined (Figure S1). IC_5, IC_{10} and IC_{20} are the concentrations most commonly used in yeast functional toxicogenomics as they allow to identify compound-specific biological responses.[20,21] At higher concentrations, non-specific cell-death effects take over, and mechanistic information is more challenging to obtain. Pools of yeast homozygous diploid deletion mutants (n = 4291) were grown with IC_5, IC_{10} and IC_{20} concentrations of gadolinium for 10 and 15 generations (six conditions in total) in an in-house built automated dispensing system robot.[24] These two generation numbers were chosen because they allow to distinguish biological effects that may be corrected over time or show delayed onset after exposure.[20,21] The strains whose growth was promoted (resistant strains) or inhibited (sensitive strains) were identified by differential strain sensitivity analysis (DSSA),[35] and their $\log_2$-fold growth change compared to controls determined (Dataset S1). **Figure 1a** shows two different trends when comparing numbers of strains affected under the different experimental conditions: at low gadolinium concentrations (IC_5), the growth of only 14 strains was disrupted after 10 and 15 generations; at IC_{10} and IC_{20}, however, the number of disrupted strains increased between 141 and 205 depending on metal concentration and generation number. Furthermore, many of the same strains were disturbed under IC_{10} and IC_{20} concentrations (**Figure 1b**). The similarities observed between IC_{10} and IC_{20} compared to IC_5 suggested that there might have been a concentration threshold, above which, the biological effects of gadolinium did not change dramatically.

The number of growth generations affected the proportion of resistant strains, where 10 generations showed higher percentage of resistant strains (36.9 ± 11.4%) than 15 generations did (16.7 ± 3.4%). Because resistant strains showed less inhibition growth (as compared to the pool of other mutants) in the presence of gadolinium, we inferred that the biological function coded by the deleted gene in the resistant mutant was directly or indirectly targeted by the metal causing toxicity, and when removed, the strain growth was less inhibited. On the other hand, sensitive strains identified genes whose deletion resulted in increased growth inhibition by the metal, and thus likely represented gene products involved in biological responses that ameliorate the metal toxicity. The larger proportion of resistant strains identified at 10 generations of exposure compared to 15 generations suggested that those toxicity-related genes

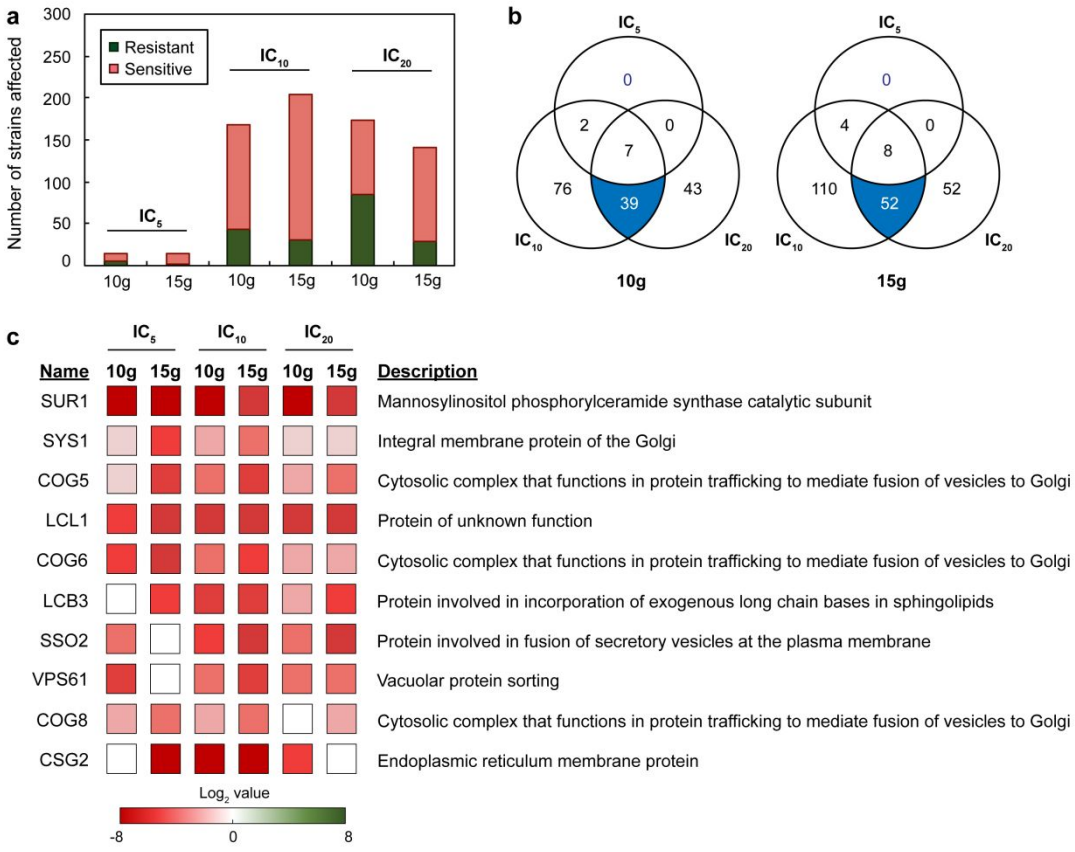

Figure 1. Sensitive and resistant strains to gadolinium identified by DSSA. (**a**) Total number of strains identified after being exposed to concentrations of gadolinium equivalent to IC_5, IC_{10}, and IC_{20} for 10 and 15 generations. (**b**) Venn diagrams of disturbed strains under different conditions. (**c**) Top genes affected by gadolinium and their growth variation in log_2 scale.

(and gene products) played important roles early on. **Figure 1c** highlights the top 10 mutants that showed growth disruption to the greatest number of experimental conditions. Although there was some variation on the biological functions of the deleted genes, four of them were related to vesicles and vesicle-mediated transport. The significance of this finding is discussed in the following sections.

We confirmed the screen results of four representative strains highlighted by DSSA (*e.g.* SUR1, COG5, FIS1 and SSO2) under non-competitive conditions on a plate reader under IC_{20} gadolinium concentrations. The mutants showed similar growth inhibitions (*i.e.* $\log_2$-fold growth variations) after gadolinium treatment under non-competitive and competitive conditions (Figure S2).

Biological attributes required for gadolinium sensitivity and resistance identified by gene ontology (GO).

GO enrichment analysis was performed with the strains highlighted by DSSA in order to identify overrepresented gene groups (known as GO terms) based on their biological characteristics.[36] Fewer numbers of overrepresented (FDR adjusted p-value < 0.05) GO terms were observed at IC_5 concentrations of gadolinium compared to IC_{10} and IC_{20} concentrations (**Figure 2**), confirming that the amount of metal under IC_5 conditions was too low to trigger significant biological responses. Notably, even though Figure 1a showed a large number of resistant strains under some specific conditions (*e.g.* IC_{20} and 10 generations), sensitive GO attributes were the predominant ones in all tested conditions (Figure 2). This observation suggested that sensitive mutations were clustered around specific biological functions, while resistant mutants were associated with a wide range of processes, since only a few resistant GO terms were statistically overrepresented. All six tested conditions were enriched with sensitive GO terms associated with transport and localization (Dataset S2), which was consistent with

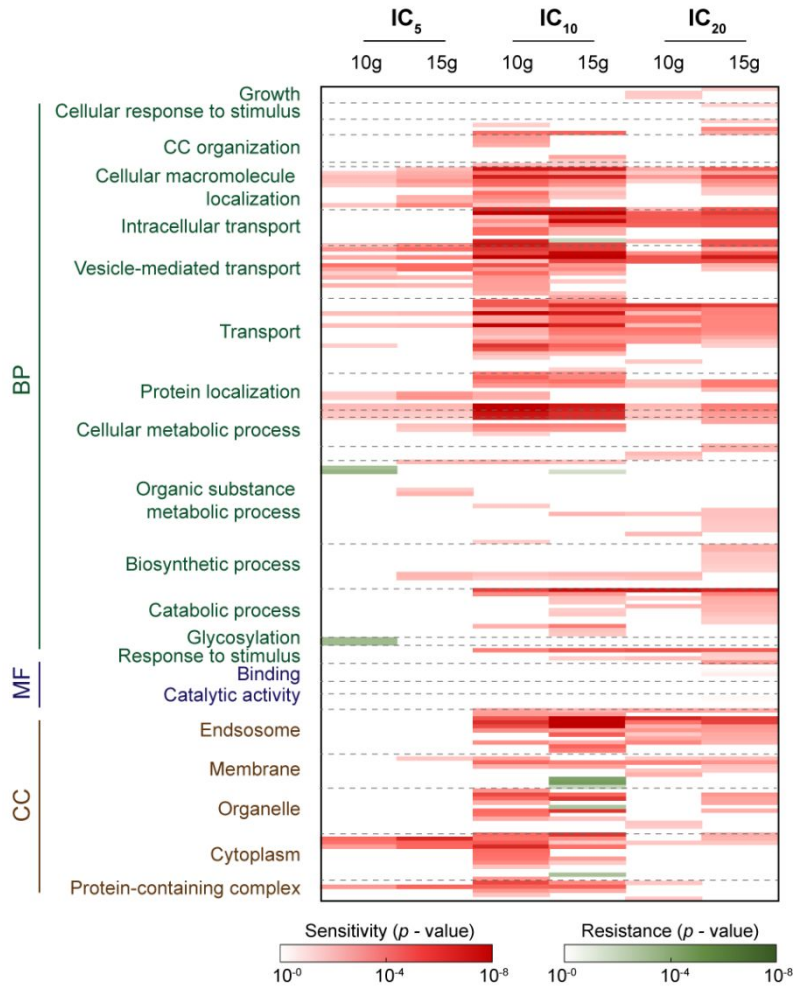

Figure 2. GO enrichment analysis of strains highlighted by DSSA. Heat map of overrepresented GO terms based on their FDR adjusted *p*-value. BP, CC and MF refer to the three GO domains: biological process, cellular component and molecular function. The cutoff was set at FDR adjusted *p*-value < 0.05

the top disturbed mutations highlighted in Figure 1c. Regarding resistant GO terms, only a few were observed, primarily associated with metabolic processes, such as glycosylation.

The predominance of transport and localization attributes was also observed among the 18 most-overrepresented GO terms, of which 7 were related to transport and 9 to localization categories (Figure S3). Moreover, four of these terms involved transport to or from the Golgi apparatus.

Pathway enrichment analysis highlighted endocytosis as the main path disturbed by gadolinium.

Pathway enrichment analysis based on the Kyoto Encyclopedia of Genes and Genomes (KEGG) database[37] was performed to further understand the impact of gadolinium on *S. cerevisiae* biological functions. This analysis took into account the functional relationships between genes and how they acted together to form specific biological pathways.[38] Three different KEGG pathways were enriched (FDR adjusted *p*-value < 0.05) among the genes highlighted by DSSA (**Figure 3**). Endocytosis was overrepresented as a sensitive pathway for all IC_{10} and IC_{20} treatments (both 10 and 15 generations), which matched the GO analysis that identified transport and vesicle-mediated transport as some of the most significant terms. The enrichment of endocytosis in the sensitive mutants indicated that disruption of endocytosis perturbed the yeast response to gadolinium toxicity. The statistical significance of this pathway became stronger (lower *p*-value and larger number of strains involved) at 15 generations, suggesting an increased importance of endocytosis with prolonged exposure. Ribosomal translation was also enriched as sensitive pathway for one treatment (IC_{10} and 10 generations) but to a lesser extent than endocytosis. KEGG pathway enrichment analysis only identified one resistant category, namely N-glycan biosynthesis, which was consistent with the resistant terms highlighted by GO analysis: organic substance metabolic process and glycosylation.

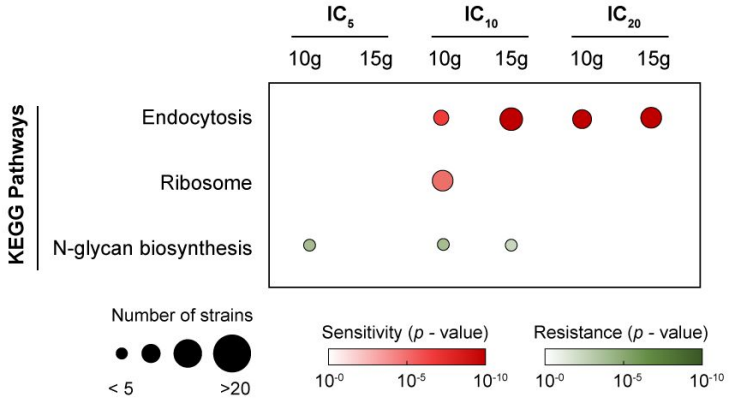

Figure 3. Pathway enrichment analysis of strains disturbed by gadolinium. The cutoff was set at FDR adjusted *p*-value < 0.05.

Clustering analysis identified the mechanism of yeast response to gadolinium, and the origin of metal toxicity

Even though GO and pathway enrichment analyses determined transport, vesicle-mediated transport, and endocytosis as some of the main functional processes required for the cellular response to gadolinium, they did not identify the corresponding action mechanism. Thus, we performed functional clustering analysis to improve the biological interpretation of our results. All genes identified by DSSA in at least two experimental conditions were grouped based on shared functional annotations (*i.e.* GO terms and KEGG pathways). The analysis was performed separately for the sensitive and the resistant strains to distinguish their contributions, and the resulting clusters displayed a list of genes with similar functionalities and their relationships with the enriched GO and KEGG terms. Three clusters that contained sensitive strains were obtained after the analysis.

The largest matrix (cluster 1 in **Figure 4a**) was a broad cluster associated with transport-related terms, while clusters 2 and 3 were more specific with functional categories related to endosome and transport to organelles (*i.e.* Golgi and vacuole), respectively. Eight of the top genes with most positive associations within the clusters 1 and 2 (*i.e.* VPS20, SNF7, SRN2, STP22, VPS28, SNF8, VSP25, and VPS36) encoded proteins that form the endosomal sorting complexes required for transport (ESCRT) system. This protein complex participates in the formation of multi-vesicular bodies (a sub-class of endosome) and protein sorting.[39] Furthermore, ESCRT machinery has also a key role in preserving yeast homeostasis by activating different responses to high concentrations of calcium;[40,41] and the deletion of certain

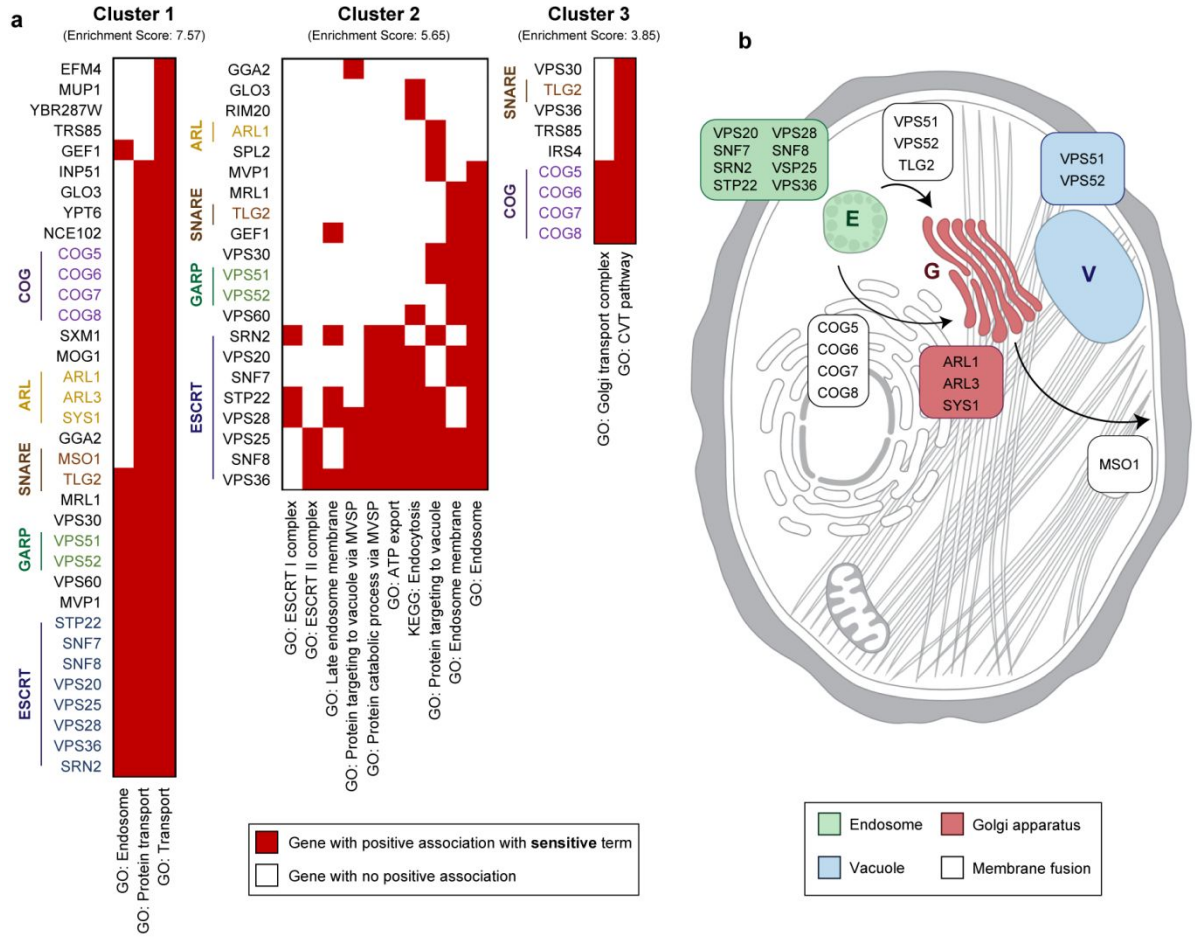

Figure 4. Cluster analysis identified the mechanisms of yeast response to gadolinium. (**a**) Clusters of sensitive genes related to vesicle-mediated transport. The following abbreviation was used in the figure: MVSP (multivesicular body sorting pathway). (**b**) Subcellular location of proteins involved in the vesicle-mediated response to gadolinium that were highlighted in clusters 1, 2 and 3. The yeast scheme was obtained with Compartments software.[32]

ESCRT proteins results in strong yeast sensitivity to calcium and higher intracellular accumulation of the cation.[40,41] Our observation that yeast used biological processes associated with calcium homeostasis in response to gadolinium treatments was consistent with lanthanides having similar coordination chemistry to calcium,[42] and competing with the cation for endogenous receptors.[43-46] Moreover, previous studies had reported that ESCRT also mediate in the yeast response to high concentrations of other metals, such as copper, cadmium, and iron.[47,48] Clusters 1 and 2 also highlighted two genes (*i.e.* VPS51 and VPS52) coding proteins of the GARP system, a tethering complex that mediates the retrograde traffic from endosomes

309 to the Golgi apparatus.[49] For instance, VPS51 in collaboration with other proteins, such as
310 TLG2 (the gene coding this protein is also in clusters 1, 2 and 3), plays a role in the membrane
311 fusion between vesicles and the Golgi, and vesicle formation in the cytoplasm to vacuole
312 targeting pathway.[50] Thus, part of the yeast response to gadolinium likely involved GARP-
313 mediated trafficking of the metal to the Golgi and the vacuole, which was consistent with the
314 reported role of these two organelles in storage and detoxification of biologically relevant
315 cations.[51,52] Similar results had been observed in *S. cerevisiae* exposed to other metallic cations,
316 such as those of aluminum, manganese, zinc, and cobalt, since mutants lacking VPS51 or
317 VPS52 were more sensitive to the metals,[53,54] and the deletion of VPS51 compromised the
318 yeast ability to discharge intracellular aluminum.[53] In addition to the aforementioned TLG2,
319 the cluster 1 also had another gene (*i.e.* MSO1) coding a protein from the SNARE family,
320 which mediates in vesicle membrane fusion.[55] Particularly, MSO1 function includes regulation
321 of membrane fusion in exocytosis sites.[56] Thus, MSO1 might have decreased the gadolinium-
322 induced stress by contributing to the metal release from the yeast cell.

323 Clusters 1 and 2 were also enriched with genes coding ARL proteins (*e.g.* ARL1 and
324 ARL3), GTPases that regulate Golgi trafficking and cytoplasm to vacuole targeting pathway.[57]
325 Moreover, ARL1 also participates in regulation of potassium influx. ARL3 activity in the Golgi
326 requires the protein SYS1,[58] whose coding gene was also highlighted in the cluster analysis.
327 Another group of genes associated with transport from or to the Golgi apparatus are COG5,
328 COG6, COG7 and COG8, which code proteins of the conserved oligomeric Golgi (COG)
329 complex. This multiprotein tethering complex (structurally similar to the GARP system) is
330 responsible for vesicle trafficking to the Golgi, and intra-Golgi trafficking.[59] Clustering
331 analysis highlighting the ARL proteins and COG complex in the yeast response to gadolinium
332 reinforced the hypothesis of the Golgi apparatus being a prominent organelle in the storage and
333 discharge of the metal. Furthermore, mutants lacking one of the COG proteins had been

reported being highly sensitive to other metals, such as cobalt and manganese.[54] Mapping the subcellular locations of the main gene products identified in clusters 1, 2 and 3 suggested some of the paths involved on the yeast response to gadolinium relied on vesicle-mediated transport through the Golgi apparatus and the vacuole prior metal discharge (**Figure 4b**).

Protein-protein interaction network analysis highlighted the protein connections involved in yeast sensitivity and resistance to gadolinium

Next, we performed protein-protein interaction network analysis to understand whether the effects of the different gadolinium treatments could be correlated to specific protein interactions. The proteins coded by the deleted genes from the strains identified by DSSA were mapped to the *S. cerevisiae* STRING database,[33] which provided clusters of protein-protein interactions. In order to distinguish the different biological effects of gadolinium, we carried out the network analysis of the top genes that promoted sensitivity (Dataset 3a) and resistance (Dataset 3b) separately.

The protein network associated with sensitive mutants was made of two sub-networks (**Figure 5a**, Table S1) and several protein pairs (Figure S4). KEGG pathway enrichment analysis of the whole network identified endocytosis as overrepresented pathway (*p*-value of $2.0 \cdot 10^{-6}$), confirming the previous GO and pathway enrichment analyses. 8 out of the 10 proteins associated with endocytosis (*i.e.* VPS20, VPS25, VPS28, VPS36, SNF7, SNF8, STP22, and RIM20) were in the highly interconnected sub-network 1, and they were part of the endosomal ESCRT system, which as previously described we identified as part of the vesicle-mediated transport response to gadolinium. Moreover, sub-network 1 also included other proteins, such as RIM8 and RIM20, which are required for the ESCRT complex function,[60] and VPS60, which mediates on the late endosome to vacuole transport.[61]

The second sub-network associated with sensitive mutants was constituted by proteins located in the Golgi apparatus (sub-network 2). These included proteins that participate in membrane fusion between vesicles and the Golgi, such as the proteins forming the COG (COG5, COG6, COG7, and COG8)[59] complex. Sub-network 2 also included two Golgi GTPases required for endosome-to-Golgi and intra-Golgi transport (YPT6),[62] and membrane trafficking and control of potassium influx (ARL1).[63,64] The last two proteins of the sub-network were a GTPase activating protein (GLO3),[65] and a membrane protein of the Golgi apparatus (SYS1).[66] Thus, protein-protein network analysis identified the Golgi apparatus as a main organelle in the yeast response to gadolinium, corroborating our previous cluster analysis (Figure 4), and it highlighted proteins involved in the fusion between vesicles and the Golgi, and in the control of cation influx as key components of the yeast detoxification pathways.

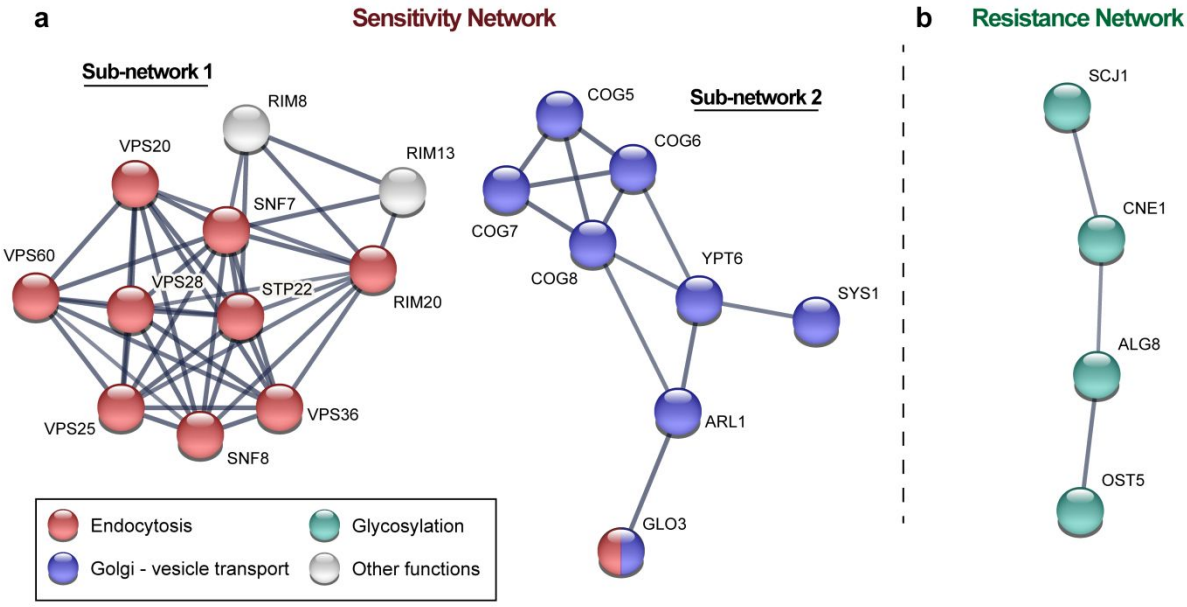

Figure 5. Protein-protein interaction network analysis identified mechanisms of gadolinium interaction with yeast. (**a**) Network of proteins coded by genes whose deletion promoted sensitivity to gadolinium. All genes affected in at least 3 experimental conditions were considered (n = 63). (**b**) Network of proteins coded by genes whose deletion promoted resistance to gadolinium. All genes affected in at least 2 experimental conditions were considered (n = 30). Proteins without connections were not displayed for clarity. The network analysis was performed with STRING and a cutoff for confidence interactions of 0.90 (highest confidence). For type of interaction evidence, refer to Figure S5.

Two protein pairs associated with sensitive mutants were related to sphingolipid biosynthesis (Figure S4). Sphingolipids are a class of lipids with sphingosine backbone that

participate in multiple regulatory mechanisms (*e.g.* endocytosis, exocytosis, calcium signaling, and environmental stress resistance) beyond their structural function as cell membrane components.[67] For instance, SUR2, one of the proteins in Figure S4 that regulates sphingolipid biosynthesis, also mediates in the trans-Golgi trafficking and exocytosis pathway.[68] Furthermore, two of the proteins in Figure S4, namely CSG2 and SLM1, interact directly or indirectly with calcium ions: CSG2 is a regulatory protein that has a binding site for calcium,[69] and mediates in the cation translocation across cell membranes, and its release;[70] SLM1, is a substrate of the Ca^{2+}-dependent calcineurin, which promotes yeast survival in environmental stress conditions through sphingolipid-mediated processes.[71] Hence, protein-protein network analysis suggested that the yeast response to gadolinium through sphingolipid-related processes might have included the modulation of vesicle-mediated transport and the repurposing of calcium regulatory processes to promote metal efflux.

The network of proteins whose deletion of corresponding genes promoted resistance (**Figure 5b**) contained 4 interconnected nodes (SCJ1, CNE1, ALG8 and OST5), which participated in glycosylation, a biosynthetic process where oligosaccharides are attached to proteins[72] that had been highlighted in our GO and pathway enrichment analyses. SCJ1 and CNE1 are both chaperones that assist in the folding and quality control of proteins[73]. SCJ1 has a Zn^{2+}-binding motif,[74,75] and CNE1 is the homolog of the mammalian Ca^{2+}-binding proteins calnexin and calrecticulin.[76] Because lanthanides have been reported to outcompete biologically-relevant metals for protein binding sites,[43-46] we hypothesized that gadolinium might have interacted with the metal binding sites of SCJ1 and CNE1, interfering with their functions and causing cytotoxicity. Furthermore, the resistant network also included two transferases (ALG8 and OST5).[77] This finding was noteworthy since gadolinium disrupting enzyme functions was consistent with previous studies that reported heavy metals binding to enzymes, mainly through cysteine residues, leading to function inhibition and yeast toxicity.[78]

Hence, network analysis suggested that gadolinium toxicity was caused by disruption of protein functions, such as enzymes and chaperones, after metal binding.

Connections between the toxicogenomic results and the pathologies associated with GBCA administration during MRI procedures

Lastly, we explored whether the genes and proteins identified in our toxicogenomic analysis could be correlated with the clinical pathologies associated with GBCA use in people. Nephrogenic systemic fibrosis (NSF) is a rare form of fibrosis, where the connective tissues of skin and internal organs thicken and scar.[79] NSF has been linked to the use of GBCAs in patients with renal dysfunction,[80] since their excretion pathways are compromised.[81] Although the exact underlying mechanism of NSF is unknown, the pathology onset is believed to be triggered by the release of the gadolinium cation from the GBCA, and its subsequent interaction with endogenous receptors.[82,83]

The top genes associated with gadolinium toxicity (highlighted in DSSA analysis as resistant strains) were screened in the Alliance of Genome Resources database,[34] and their human orthologues identified (Table S2). 32 conserved genes and their proteins were obtained, suggesting that they may play a role in gadolinium toxicity in humans. Moreover, alterations in 12 of these genes have been correlated to different types of fibroses (please refer to Table S2 for the full list). For instance, functional disruptions in the genes coding the Ca^{2+}-binding proteins calreticulin (CALR) and calmegin (CLGN) are linked to myelofibrosis and kidney fibrosis, respectively.[84,85] Mutations of AP1S1 (*i.e.* a gene that codes a subunit of the AP1 protein that is involved in endocytosis and Golgi processing) affect intracellular copper metabolism, resulting on MEDNIK syndrome and hepatic fibrosis.[86] In addition, the functional loss of AP1S3, a gene coding another AP1 subunit, is associated with skin autoinflammation by keratinocyte autophagy disruption.[87] YPEL 4 is another human orthologue highlighted in our analysis that contains a putative zinc-finger-like metal-binding site, whose mutation has

been linked to lung fibrosis through signal transduction pathway malfunction.[88] Although fibrosis can occur in a wide range of organs with different pathological origins, several of the ones previously described involve disruptions of cation-binding proteins and metal metabolism. Thus, those may also be involved in the onset of NSF after GBCA administration in patients with renal dysfunction.

Identifying gadolinium endogenous targets may also offer opportunities for developing prophylactic and therapeutic strategies against NSF. As an example, our analysis identified TOR1 and its gene product as gadolinium targets associated with metal toxicity in yeast (Table S2). Its human orthologue is mTOR, whose overactivation has been linked to heart and pulmonary fibroses, among others.[89,90] Experiments with transgenic mice that had overactivated mTOR showed the *in vivo* models developing heart fibrosis.[91] Nevertheless, administration of sirolimus, a mTOR inhibitor, suppressed interstitial fibrosis in the heart tissues. A subsequent study compared sirolimus with everolimus (another mTOR inhibitor), and both chemicals decreased fibrosis up to 70% after 5 weeks in rats.[92] Hence, if the genes and proteins shown in Table S2 are confirmed to play a role in gadolinium-induced toxicity in humans, as we proved they do in yeast, prophylactic treatments using function modulating drugs, such as inhibitors, may decrease the metal toxicity and prevent NSF development.

Conclusions

In summary, we have identified the biological functions involved in gadolinium toxicity in *S. cerevisiae,* as well as the cellular response mechanisms. Gadolinium effects had a concentration threshold, with a low number of strains identified at IC_5 concentrations, while a larger number of mutants were identified at IC_{10} and IC_{20} concentrations. Multidimensional analysis showed that the yeast response to the metal was time dependent, involving more gene

product as the time of exposure increased. Vesicle-mediated transport and endocytosis were highlighted by GO and pathway enrichment analyses as the main biological responses involved in protection against gadolinium toxicity, while cytotoxicity was likely related to the disruption of metabolic processes, such as glycosylation. Cluster analysis and protein-protein interaction network analysis linked the yeast response to different proteins involved in vesicle-mediated transport through the Golgi apparatus and the vacuole, and subsequent exocytosis. Several of these proteins were involved in the regulation of biologically-relevant cations, such as calcium ions, suggesting that the yeast repurposed these regulatory processes to promote gadolinium efflux. Network analysis also supported our hypothesis that gadolinium disrupted the function of specific metabolic enzymes and chaperones, which may underlie yeast cytotoxicity. Lastly, several of the genes and proteins highlighted in our analyses are conserved in humans and their disruption has been linked to fibrosis, suggesting that they may also participate in gadolinium-induced NSF onset. Therefore, identification of gadolinium targets is critical in the future development of therapeutic and prophylactic strategies to decrease NSF adverse health effects in patients.

ASSOCIATED CONTENT

Supporting Information.

Determination of IC_5, IC_{10} and IC_{20} concentrations of gadolinium; non-competitive growth of representative mutants under IC_{20} concentrations of gadolinium; Human orthologues of genes associated with gadolinium toxicity.

Notes

The authors declare no competing financial interest.

AUTHOR INFORMATION

Corresponding Author. *E-mail: abergel@berkeley.edu.

ORCID

Roger M. Pallares: 0000-0001-7423-8706

Dahlia D. An: 0000-0002-8763-6735

David Faulkner: 0000-0001-5532-2304

Rebecca J. Abergel: 0000-0002-3906-8761

ACKNOWLEDGMENTS

The experimental work was supported by the Laboratory Directed Research and Development Program at the Lawrence Berkeley National Laboratory (LBNL), operating under U.S. Department of Energy (DOE) Contract No. DE-AC02-05CH11231. Final analysis and assembly of the manuscript was made possible by a grant from the Berkeley Lab Foundation.

References

(1) Cotton, S. Introduction to the Lanthanides. In *Lanthanide and Actinide Chemistry*; John Wiley & Sons: Hoboken, NJ, 2006; pp 1-7.
(2) Caravan, P. Strategies for increasing the sensitivity of gadolinium based MRI contrast agents. *Chem. Soc. Rev.* **2006,** *35* (6), 512-523.
(3) Zhou, Z.; Lu, Z.-R. Gadolinium-based contrast agents for magnetic resonance cancer imaging. *Wiley Interdisciplinary Reviews: Nanomedicine and Nanobiotechnology* **2013,** *5* (1), 1-18.
(4) Glover, G. H. Overview of functional magnetic resonance imaging. *Neurosurg Clin N Am* **2011,** *22* (2), 133-vii.
(5) Tóth, é.; Helm, L.; Merbach, A. Relaxivity of Gadolinium(III) Complexes: Theory and Mechanism. In *The Chemistry of Contrast Agents in Medical Magnetic Resonance Imaging*; Wiley Hoboken, NJ, 2013; pp 25-81.
(6) Lohrke, J.; Frenzel, T.; Endrikat, J.; Alves, F. C.; Grist, T. M.; Law, M.; Lee, J. M.; Leiner, T.; Li, K.-C.; Nikolaou, K.; Prince, M. R.; Schild, H. H.; Weinreb, J. C.; Yoshikawa, K.; Pietsch, H. 25 Years of Contrast-Enhanced MRI: Developments, Current Challenges and Future Perspectives. *Advances in Therapy* **2016,** *33* (1), 1-28.
(7) Grobner, T. Gadolinium – a specific trigger for the development of nephrogenic fibrosing dermopathy and nephrogenic systemic fibrosis? *Nephrology Dialysis Transplantation* **2006,** *21* (4), 1104-1108.
(8) Kuo, P. H.; Kanal, E.; Abu-Alfa, A. K.; Cowper, S. E. Gadolinium-based MR Contrast Agents and Nephrogenic Systemic Fibrosis. *Radiology* **2007,** *242* (3), 647-649.
(9) Kanda, T.; Oba, H.; Toyoda, K.; Kitajima, K.; Furui, S. Brain gadolinium deposition after administration of gadolinium-based contrast agents. *Japanese Journal of Radiology* **2016,** *34* (1), 3-9.
(10) Robert, P.; Violas, X.; Grand, S.; Lehericy, S.; Idée, J.-M.; Ballet, S.; Corot, C. Linear Gadolinium-Based Contrast Agents Are Associated With Brain Gadolinium Retention in Healthy Rats. *Invest Radiol* **2016,** *51* (2), 73-82.
(11) FDA Drug Safety Communication: FDA evaluating the risk of brain deposits with repeated use of gadolinium-based contrast agents for magnetic resonance imaging (MRI). U.S. Food and Drug Administration: 2017.
(12) Dekkers, I. A.; Roos, R.; van der Molen, A. J. Gadolinium retention after administration of contrast agents based on linear chelators and the recommendations of the European Medicines Agency. *European Radiology* **2018,** *28* (4), 1579-1584.
(13) Pallares, R. M.; An, D. D.; Tewari, P.; Wang, E. T.; Abergel, R. J. Rapid Detection of Gadolinium-Based Contrast Agents in Urine with a Chelated Europium Luminescent Probe. *ACS Sensors* **2020,** *5* (5), 1281-1286.
(14) Pallares, R. M.; Carter, K. P.; Zeltmann, S. E.; Tratnjek, T.; Minor, A. M.; Abergel, R. J. Selective Lanthanide Sensing with Gold Nanoparticles and Hydroxypyridinone Chelators. *Inorg. Chem.* **2020,** *59* (3), 2030-2036.
(15) Rees, J. A.; Deblonde, G. J. P.; An, D. D.; Ansoborlo, C.; Gauny, S. S.; Abergel, R. J. Evaluating the potential of chelation therapy to prevent and treat gadolinium deposition from MRI contrast agents. *Sci. Rep.* **2018,** *8* (1), 4419.
(16) González, V.; Vignati, D. A. L.; Pons, M.-N.; Montarges-Pelletier, E.; Bojic, C.; Giamberini, L. Lanthanide ecotoxicity: First attempt to measure environmental risk for aquatic organisms. *Environ. Pollut.* **2015,** *199*, 139-147.
(17) Blasco-Perrin, H.; Glaser, B.; Pienkowski, M.; Peron, J. M.; Payen, J. L. Gadolinium induced recurrent acute pancreatitis. *Pancreatology* **2013,** *13* (1), 88-89.

(18) Terzi, C.; Sökmen, S. Acute pancreatitis induced by magnetic-resonance-imaging contrast agent. *The Lancet* **1999,** *354* (9192), 1789-1790.
(19) Giaever, G.; Nislow, C. The Yeast Deletion Collection: A Decade of Functional Genomics. *Genetics* **2014,** *197* (2), 451.
(20) Gaytán, B. D.; Loguinov, A. V.; Peñate, X.; Lerot, J.-M.; Chávez, S.; Denslow, N. D.; Vulpe, C. D. A Genome-Wide Screen Identifies Yeast Genes Required for Tolerance to Technical Toxaphene, an Organochlorinated Pesticide Mixture. *PLoS One* **2013,** *8* (11), e81253.
(21) North, M.; Tandon, V. J.; Thomas, R.; Loguinov, A.; Gerlovina, I.; Hubbard, A. E.; Zhang, L.; Smith, M. T.; Vulpe, C. D. Genome-Wide Functional Profiling Reveals Genes Required for Tolerance to Benzene Metabolites in Yeast. *PLoS One* **2011,** *6* (8), e24205.
(22) Pallares, R. M.; Faulkner, D.; An, D. D.; Hébert, S.; Loguinov, A.; Proctor, M.; Villalobos, J. A.; Bjornstad, K. A.; Rosen, C. J.; Vulpe, C.; Abergel, R. J. Genome-wide toxicogenomic study of the lanthanides sheds light on the selective toxicity mechanisms associated with critical materials. *Proc. Natl. Acad. Sci.* **2021,** *118* (18), e2025952118.
(23) Pallares, R. M.; An, D. D.; Hébert, S.; Faulkner, D.; Loguinov, A.; Proctor, M.; Villalobos, J. A.; Bjornstad, K. A.; Rosen, C. J.; Vulpe, C.; Abergel, R. J. Multidimensional genome-wide screening in yeast provides mechanistic insights into europium toxicity. *Metallomics* **2021,** *13* (12), mfab061.
(24) Proctor, M.; Urbanus, M. L.; Fung, E. L.; Jaramillo, D. F.; Davis, R. W.; Nislow, C.; Giaever, G. The Automated Cell: Compound and Environment Screening System (ACCESS) for Chemogenomic Screening. In *Yeast Systems Biology: Methods and Protocols*; Castrillo, J. I.; Oliver, S. G., Eds.; Humana Press: Totowa, NJ, 2011; pp 239-269.
(25) Andrews, S. *FastQC: A quality control tool for high throughput sequence data.*, 0.10; Babraham Bioinformatics: Cambridge, UK, 2011.
(26) Gordon, A.; Hannon, G. J. *Fastx-toolkit*, 2010.
(27) Pagès, H.; Aboyoun, P.; Gentleman, R.; DebRoy, S. *Biostrings: Efficient manipulation of biological strings*, 2017.
(28) Love, M. I.; Huber, W.; Anders, S. Moderated estimation of fold change and dispersion for RNA-seq data with DESeq2. *Genome Biology* **2014,** *15* (12), 550.
(29) Dennis, G.; Sherman, B. T.; Hosack, D. A.; Yang, J.; Gao, W.; Lane, H. C.; Lempicki, R. A. DAVID: Database for Annotation, Visualization, and Integrated Discovery. *Genome Biology* **2003,** *4* (9), R60.
(30) Storey, J. D. A direct approach to false discovery rates. *Journal of the Royal Statistical Society: Series B (Statistical Methodology)* **2002,** *64* (3), 479-498.
(31) The UniProt, C. UniProt: a hub for protein information. *Nucleic Acids Res.* **2015,** *43* (D1), D204-D212.
(32) Binder, J. X.; Pletscher-Frankild, S.; Tsafou, K.; Stolte, C.; O'Donoghue, S. I.; Schneider, R.; Jensen, L. J. COMPARTMENTS: unification and visualization of protein subcellular localization evidence. *Database* **2014,** *2014*.
(33) Szklarczyk, D.; Franceschini, A.; Wyder, S.; Forslund, K.; Heller, D.; Huerta-Cepas, J.; Simonovic, M.; Roth, A.; Santos, A.; Tsafou, K. P.; Kuhn, M.; Bork, P.; Jensen, L. J.; von Mering, C. STRING v10: protein–protein interaction networks, integrated over the tree of life. *Nucleic Acids Res.* **2014,** *43* (D1), D447-D452.
(34) The Alliance of Genome Resources, C. Alliance of Genome Resources Portal: unified model organism research platform. *Nucleic Acids Res.* **2020,** *48* (D1), D650-D658.
(35) Jo, W. J.; Loguinov, A.; Wintz, H.; Chang, M.; Smith, A. H.; Kalman, D.; Zhang, L.; Smith, M. T.; Vulpe, C. D. Comparative Functional Genomic Analysis Identifies Distinct and Overlapping Sets of Genes Required for Resistance to Monomethylarsonous Acid (MMAIII) and Arsenite (AsIII) in Yeast. *Toxicol. Sci.* **2009,** *111* (2), 424-436.

(36) Eden, E.; Navon, R.; Steinfeld, I.; Lipson, D.; Yakhini, Z. GOrilla: a tool for discovery and visualization of enriched GO terms in ranked gene lists. *BMC Bioinformatics* **2009,** *10* (1), 48.
(37) Kanehisa, M.; Goto, S. KEGG: Kyoto Encyclopedia of Genes and Genomes. *Nucleic Acids Res.* **2000,** *28* (1), 27-30.
(38) Reimand, J.; Isserlin, R.; Voisin, V.; Kucera, M.; Tannus-Lopes, C.; Rostamianfar, A.; Wadi, L.; Meyer, M.; Wong, J.; Xu, C.; Merico, D.; Bader, G. D. Pathway enrichment analysis and visualization of omics data using g:Profiler, GSEA, Cytoscape and EnrichmentMap. *Nat. Protoc.* **2019,** *14* (2), 482-517.
(39) Saksena, S.; Sun, J.; Chu, T.; Emr, S. D. ESCRTing proteins in the endocytic pathway. *Trends Biochem. Sci.* **2007,** *32* (12), 561-573.
(40) Zhao, Y.; Du, J.; Xiong, B.; Xu, H.; Jiang, L. ESCRT components regulate the expression of the ER/Golgi calcium pump gene PMR1 through the Rim101/Nrg1 pathway in budding yeast. *Journal of Molecular Cell Biology* **2013,** *5* (5), 336-344.
(41) Bowers, K.; Lottridge, J.; Helliwell, S. B.; Goldthwaite, L. M.; Luzio, J. P.; Stevens, T. H. Protein–Protein Interactions of ESCRT Complexes in the Yeast Saccharomyces cerevisiae. *Traffic* **2004,** *5* (3), 194-210.
(42) Cotruvo, J. A. The Chemistry of Lanthanides in Biology: Recent Discoveries, Emerging Principles, and Technological Applications. *ACS Central Science* **2019,** *5* (9), 1496-1506.
(43) Brayshaw, L. L.; Smith, R. C. G.; Badaoui, M.; Irving, J. A.; Price, S. R. Lanthanides compete with calcium for binding to cadherins and inhibit cadherin-mediated cell adhesion. *Metallomics* **2019,** *11* (5), 914-924.
(44) Edington, S. C.; Gonzalez, A.; Middendorf, T. R.; Halling, D. B.; Aldrich, R. W.; Baiz, C. R. Coordination to lanthanide ions distorts binding site conformation in calmodulin. *Proc. Natl. Acad. Sci.* **2018,** *115* (14), E3126.
(45) Pallares, R. M.; Panyala, N. R.; Sturzbecher-Hoehne, M.; Illy, M.-C.; Abergel, R. J. Characterizing the general chelating affinity of serum protein fetuin for lanthanides. *J. Biol. Inorg. Chem.* **2020,** *25* (7), 941-948.
(46) Itoh, N.; Kawakita, M. Characterization of Gd 3+ and Tb 3+ Binding Sites on Ca 2+ , Mg 2+ -Adenosine Triphosphatase of Sarcoplasmic Reticulum 1. *The Journal of Biochemistry* **1984,** *95* (3), 661-669.
(47) Jo, W. J.; Loguinov, A.; Chang, M.; Wintz, H.; Nislow, C.; Arkin, A. P.; Giaever, G.; Vulpe, C. D. Identification of Genes Involved in the Toxic Response of Saccharomyces cerevisiae against Iron and Copper Overload by Parallel Analysis of Deletion Mutants. *Toxicol. Sci.* **2007,** *101* (1), 140-151.
(48) Serero, A.; Lopes, J.; Nicolas, A.; Boiteux, S. Yeast genes involved in cadmium tolerance: Identification of DNA replication as a target of cadmium toxicity. *DNA Repair* **2008,** *7* (8), 1262-1275.
(49) Eising, S.; Thiele, L.; Fröhlich, F. A systematic approach to identify recycling endocytic cargo depending on the GARP complex. *eLife* **2019,** *8*, e42837.
(50) Reggiori, F.; Wang, C.-W.; Stromhaug, P. E.; Shintani, T.; Klionsky, D. J. Vps51 Is Part of the Yeast Vps Fifty-three Tethering Complex Essential for Retrograde Traffic from the Early Endosome and Cvt Vesicle Completion. *J. Biol. Chem.* **2003,** *278* (7), 5009-5020.
(51) Reddi, A. R.; Jensen, L. T.; Culotta, V. C. Manganese Homeostasis in Saccharomyces cerevisiae. *Chem. Rev.* **2009,** *109* (10), 4722-4732.
(52) Liu, W. Control of Calcium in Yeast Cells. In *Introduction to Modeling Biological Cellular Control Systems*; Liu, W., Ed.; Springer Milan: Milano, 2012; pp 95-122.
(53) Kakimoto, M.; Kobayashi, A.; Fukuda, R.; Ono, Y.; Ohta, A.; Yoshimura, E. Genome-Wide Screening of Aluminum Tolerance in Saccharomyces cerevisiae. *BioMetals* **2005,** *18* (5), 467-474.

(54) Bleackley, M. R.; Young, B. P.; Loewen, C. J. R.; MacGillivray, R. T. A. High density array screening to identify the genetic requirements for transition metal tolerance in Saccharomyces cerevisiae. *Metallomics* **2011,** *3* (2), 195-205.
(55) Burri, L.; Lithgow, T. A Complete Set of SNAREs in Yeast. *Traffic* **2004,** *5* (1), 45-52.
(56) Weber, M.; Chernov, K.; Turakainen, H.; Wohlfahrt, G.; Pajunen, M.; Savilahti, H.; Jäntti, J. Mso1p Regulates Membrane Fusion through Interactions with the Putative N-Peptide–binding Area in Sec1p Domain 1. *Mol. Biol. Cell* **2010,** *21* (8), 1362-1374.
(57) Jackson, C. L. Membrane Traffic: Arl GTPases Get a GRIP on the Golgi. *Curr. Biol.* **2003,** *13* (5), R174-R176.
(58) Setty, S. R. G.; Strochlic, T. I.; Tong, A. H. Y.; Boone, C.; Burd, C. G. Golgi targeting of ARF-like GTPase Arl3p requires its Nα-acetylation and the integral membrane protein Sys1p. *Nat. Cell Biol.* **2004,** *6* (5), 414-419.
(59) Whyte, J. R. C.; Munro, S. Vesicle tethering complexes in membrane traffic. *J. Cell Sci.* **2002,** *115* (13), 2627.
(60) Boysen, J. H.; Mitchell, A. P. Control of Bro1-Domain Protein Rim20 Localization by External pH, ESCRT Machinery, and the Saccharomyces cerevisiae Rim101 Pathway. *Mol. Biol. Cell* **2006,** *17* (3), 1344-1353.
(61) Köhler, J. R. Mos10 (Vps60) is required for normal filament maturation in Saccharomyces cerevisiae. *Mol. Microbiol.* **2003,** *49* (5), 1267-1285.
(62) Suda, Y.; Kurokawa, K.; Hirata, R.; Nakano, A. Rab GAP cascade regulates dynamics of Ypt6 in the Golgi traffic. *Proc. Natl. Acad. Sci.* **2013,** *110* (47), 18976.
(63) Rosenwald, A. G.; Rhodes, M. A.; Van Valkenburgh, H.; Palanivel, V.; Chapman, G.; Boman, A.; Zhang, C.-j.; Kahn, R. A. ARL1 and membrane traffic in Saccharomyces cerevisiae. *Yeast* **2002,** *19* (12), 1039-1056.
(64) Munson, A. M.; Haydon, D. H.; Love, S. L.; Fell, G. L.; Palanivel, V. R.; Rosenwald, A. G. Yeast ARL1 encodes a regulator of K+ influx. *J. Cell Sci.* **2004,** *117* (11), 2309.
(65) Dogic, D.; De Chassey, B.; Pick, E.; Cassel, D.; Lefkir, Y.; Hennecke, S.; Cosson, P.; Letourneur, F. The ADP-ribosylation factor GTPase-activating protein GIo3p is involved in ER retrieval. *Eur. J. Cell Biol.* **1999,** *78* (5), 305-310.
(66) Votsmeier, C.; Gallwitz, D. An acidic sequence of a putative yeast Golgi membrane protein binds COPII and facilitates ER export. *The EMBO Journal* **2001,** *20* (23), 6742-6750.
(67) Dickson, R. C. Roles for Sphingolipids in Saccharomyces cerevisiae. In *Sphingolipids as Signaling and Regulatory Molecules*; Chalfant, C.; Poeta, M. D., Eds.; Springer New York: New York, NY, 2010; pp 217-231.
(68) Proszynski, T. J.; Klemm, R. W.; Gravert, M.; Hsu, P. P.; Gloor, Y.; Wagner, J.; Kozak, K.; Grabner, H.; Walzer, K.; Bagnat, M.; Simons, K.; Walch-Solimena, C. A genome-wide visual screen reveals a role for sphingolipids and ergosterol in cell surface delivery in yeast. *Proc. Natl. Acad. Sci. U. S. A.* **2005,** *102* (50), 17981.
(69) Uemura, S.; Kihara, A.; Iwaki, S.; Inokuchi, J.-i.; Igarashi, Y. Regulation of the Transport and Protein Levels of the Inositol Phosphorylceramide Mannosyltransferases Csg1 and Csh1 by the Ca2+-binding Protein Csg2. *J. Biol. Chem.* **2007,** *282* (12), 8613-8621.
(70) Beeler, T.; Gable, K.; Zhao, C.; Dunn, T. A novel protein, CSG2p, is required for Ca2+ regulation in Saccharomyces cerevisiae. *J. Biol. Chem.* **1994,** *269* (10), 7279-7284.
(71) Bultynck, G.; Heath, V. L.; Majeed, A. P.; Galan, J.-M.; Haguenauer-Tsapis, R.; Cyert, M. S. Slm1 and Slm2 Are Novel Substrates of the Calcineurin Phosphatase Required for Heat Stress-Induced Endocytosis of the Yeast Uracil Permease. *Mol. Cell. Biol.* **2006,** *26* (12), 4729.
(72) Poljak, K.; Selevsek, N.; Ngwa, E.; Grossmann, J.; Losfeld, M. E.; Aebi, M. Quantitative Profiling of N-linked Glycosylation Machinery in Yeast Saccharomyces cerevisiae. *Mol. Cell. Proteomics* **2018,** *17* (1), 18.

(73) Buck, T. M.; Wright, C. M.; Brodsky, J. L. The activities and function of molecular chaperones in the endoplasmic reticulum. *Seminars in Cell & Developmental Biology* **2007,** *18* (6), 751-761.
(74) Silberstein, S.; Schlenstedt, G.; Silver, P. A.; Gilmore, R. A Role for the DnaJ Homologue Scj1p in Protein Folding in the Yeast Endoplasmic Reticulum. *J. Cell Biol.* **1998,** *143* (4), 921-933.
(75) Ellis, C. D.; Wang, F.; MacDiarmid, C. W.; Clark, S.; Lyons, T.; Eide, D. J. Zinc and the Msc2 zinc transporter protein are required for endoplasmic reticulum function. *J. Cell Biol.* **2004,** *166* (3), 325-335.
(76) De Virgilio, C.; Bürckert, N.; Neuhaus, J.-M.; Boller, T.; Wiemken, A. CNE1, a Saccharomyces cerevisiae Homologue of the Genes Encoding Mammalian Calnexin and Calreticulin. *Yeast* **1993,** *9* (2), 185-188.
(77) Larkin, A.; Imperiali, B. The Expanding Horizons of Asparagine-Linked Glycosylation. *Biochemistry* **2011,** *50* (21), 4411-4426.
(78) Wysocki, R.; Tamás, M. J. How Saccharomyces cerevisiae copes with toxic metals and metalloids. *FEMS Microbiol. Rev.* **2010,** *34* (6), 925-951.
(79) Kaewlai, R.; Abujudeh, H. Nephrogenic Systemic Fibrosis. *American Journal of Roentgenology* **2012,** *199* (1), W17-W23.
(80) Marckmann, P.; Skov, L.; Rossen, K.; Dupont, A.; Damholt, M. B.; Heaf, J. G.; Thomsen, H. S. Nephrogenic Systemic Fibrosis: Suspected Causative Role of Gadodiamide Used for Contrast-Enhanced Magnetic Resonance Imaging. *Journal of the American Society of Nephrology* **2006,** *17* (9), 2359.
(81) Aime, S.; Caravan, P. Biodistribution of gadolinium-based contrast agents, including gadolinium deposition. *Journal of Magnetic Resonance Imaging* **2009,** *30* (6), 1259-1267.
(82) Morcos, S. K. Nephrogenic systemic fibrosis following the administration of extracellular gadolinium based contrast agents: is the stability of the contrast agent molecule an important factor in the pathogenesis of this condition? *The British Journal of Radiology* **2007,** *80* (950), 73-76.
(83) Idée, J.-M.; Fretellier, N.; Robic, C.; Corot, C. The role of gadolinium chelates in the mechanism of nephrogenic systemic fibrosis: A critical update. *Critical Reviews in Toxicology* **2014,** *44* (10), 895-913.
(84) Diamond, J. M. S.; de Almeida, A. M.; Belo, H. J. L. M. R.; da Costa, M. P. G. P. G.; Cabeçadas, J. M. V. S.; Abecasis, M. M. d. S. F. CALR-mutated primary myelofibrosis evolving to chronic myeloid leukemia with both CALR mutation and BCR-ABL1 fusion gene. *Annals of Hematology* **2016,** *95* (12), 2101-2104.
(85) Trivedi, P.; Kumar, R. K.; Iyer, A.; Boswell, S.; Gerarduzzi, C.; Dadhania, V. P.; Herbert, Z.; Joshi, N.; Luyendyk, J. P.; Humphreys, B. D.; Vaidya, V. S. Targeting Phospholipase D4 Attenuates Kidney Fibrosis. *Journal of the American Society of Nephrology* **2017,** *28* (12), 3579.
(86) Martinelli, D.; Travaglini, L.; Drouin, C. A.; Ceballos-Picot, I.; Rizza, T.; Bertini, E.; Carrozzo, R.; Petrini, S.; de Lonlay, P.; El Hachem, M.; Hubert, L.; Montpetit, A.; Torre, G.; Dionisi-Vici, C. MEDNIK syndrome: a novel defect of copper metabolism treatable by zinc acetate therapy. *Brain* **2013,** *136* (3), 872-881.
(87) Mahil, S. K.; Twelves, S.; Farkas, K.; Setta-Kaffetzi, N.; Burden, A. D.; Gach, J. E.; Irvine, A. D.; Képíró, L.; Mockenhaupt, M.; Oon, H. H.; Pinner, J.; Ranki, A.; Seyger, M. M. B.; Soler-Palacin, P.; Storan, E. R.; Tan, E. S.; Valeyrie-Allanore, L.; Young, H. S.; Trembath, R. C.; Choon, S.-E.; Szell, M.; Bata-Csorgo, Z.; Smith, C. H.; Di Meglio, P.; Barker, J. N.; Capon, F. AP1S3 Mutations Cause Skin Autoinflammation by Disrupting Keratinocyte Autophagy and Up-Regulating IL-36 Production. *J. Invest. Dermatol.* **2016,** *136* (11), 2251-2259.

(88) Truong, L.; Zheng, Y.-M.; Song, T.; Tang, Y.; Wang, Y.-X. Potential important roles and signaling mechanisms of YPEL4 in pulmonary diseases. *Clinical and Translational Medicine* **2018,** *7* (1), 16.
(89) Samidurai, A.; Kukreja, R. C.; Das, A. Emerging Role of mTOR Signaling-Related miRNAs in Cardiovascular Diseases. *Oxidative Medicine and Cellular Longevity* **2018,** *2018*, 6141902.
(90) Lawrence, J.; Nho, R. The Role of the Mammalian Target of Rapamycin (mTOR) in Pulmonary Fibrosis. *Int. J. Mol. Sci.* **2018,** *19* (3), 778.
(91) Lian, H.; Ma, Y.; Feng, J.; Dong, W.; Yang, Q.; Lu, D.; Zhang, L. Heparin-Binding EGF-Like Growth Factor Induces Heart Interstitial Fibrosis via an Akt/mTor/p70s6k Pathway. *PLoS One* **2012,** *7* (9), e44946.
(92) Patsenker, E.; Schneider, V.; Ledermann, M.; Saegesser, H.; Dorn, C.; Hellerbrand, C.; Stickel, F. Potent antifibrotic activity of mTOR inhibitors sirolimus and everolimus but not of cyclosporine A and tacrolimus in experimental liver fibrosis. *Journal of Hepatology* **2011,** *55* (2), 388-398.